

PAPER REF: 7309

## **ON THE USE OF RADAR INTERFEROMETRY FOR THE STRUCTURAL MONITORING OF BRIDGES**

**Rui C. Barros<sup>1(\*)</sup>, Fabio M. Paiva<sup>2</sup>**

<sup>1</sup>Dept of Civil Engineering (Structural Division), FEUP, University of Porto, Portugal

<sup>2</sup>Instituto Superior Tecnico (IST, Lisbon), Infrarisk Program grantee (IST-FEUP), Portugal

(\*)*Email: rcb@fe.up.pt*

### **ABSTRACT**

This work constitutes a synthesis of the cumulative experience at Faculdade Engenharia Universidade do Porto (FEUP) on the structural health monitoring (SHM) of four bridges in Portugal, of different bridge typologies and materials: a stress-ribbon footbridge, a metallic roadway bridge, a mixed construction railway bridge, and a centennial metallic one-way bridge. After a simple technical introduction of this non-intrusive SHM technique, the work is mainly devoted to the description and observations of the three bridge situations mentioned above, which constitute three case studies. Thereafter, for each case study is described the evaluation of results with such technical equipment, as well as the comparison with akin results obtained for the same case studies either by structural computational modelling or by other intrusive SHM techniques, in order to ascertain the accuracy of this non-intrusive radar interferometry method.

**Keywords:** SHM, radar interferometry, bridge dynamics.

### **INTRODUCTION**

Some experience in using radar interferometry (RI) for SHM of general structures was initiated in 2013 at FEUP by a research team led by first co-author, in the context of the R&D collaborative project VHSS-Poles (Metalgalva Group and FEUP) sponsored by *EU Compete program* (Barros, 2015).

Although initially applied to the observation and SHM of towers and pole-like structures (telecommunication towers, stacks, transmission towers and poles or posts) it immediately proved its versatility in several circumstances ranging from laboratory monitoring of dynamic tests to the more general case of SHM of bridges.

### **RADAR TECHNICAL CHARACTERISTICS**

The radar sensor (Figure1) used in this work (IDS, IBIS-FS system) is an industrially engineered micro-wave interferometer and consists of a sensor module, a control PC and a power supply unit. For a more comprehensive description on the technical features of the radar the reader is referred to (Silva, 2015) and (Gentile, 2010-2011).

The measurement of deflections follows two main steps (Silva, 2015): (a) to employ a radar to take coherent and consecutive images of the investigated structure, with each image being a distance map of the radar echoes intensity coming from the reflecting targets detected on the

structure; (b) to compute the displacement of each target by comparing the phase information of the back-scattered electromagnetic waves collected at different times.



Fig. 1 - View of the radar interferometer from (Silva, 2015).

## CASE STUDIES

A total of three case studies will be presented in the present section: FEUP Stress-Ribbon Footbridge (case A); Pinhão Bridge (case B), and Alcacer-do-Sal Railway Bridge (case C).

### A- FEUP Stress-Ribbon Footbridge

#### Structural Description

The geometric description of FEUP stress-ribbon footbridge is shown in Figure 2, taken directly from the project design data report (Caetano, 2010).

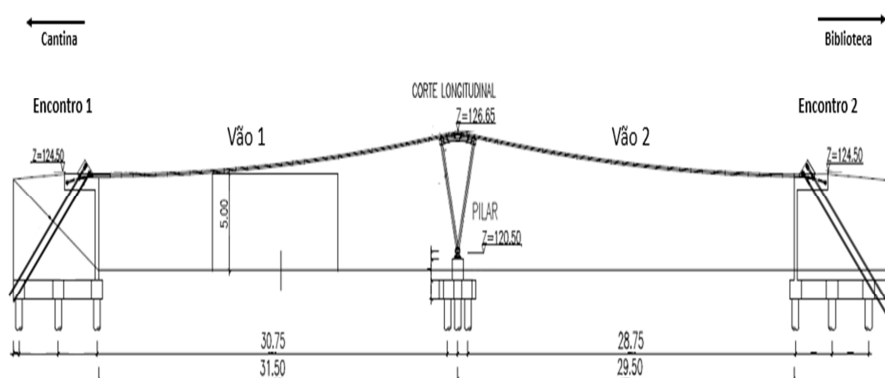


Fig. 2 - Front view of the stress-ribbon footbridge (dimensions in m) from (Silva, 2015) and (Caetano, 2010).

The bridge has a total length of 61 meters, corresponding 30 meters to the first span (southbound) and 28 meters to the second span (northbound).

The zone of the central support has a total length of 3 meters, 1.5 meters for each side. Throughout its length, the bridge deck is a sequence of pre-slabs of rectangular cross section with area  $3.80 \times 0.15$  m<sup>2</sup>, distributed evenly every 1 meter. For the connection between the pre-slabs, were used concrete joints with cross section of  $3.80 \times 0.034$  m<sup>2</sup>. Each cross section contains 4 cables with  $7\phi 15.2$  mm wire (Silva, 2015) and (Caetano, 2010).

The central support, shown in Figure 2 and Figure 3, has 4 tubular steel columns (S 355) with diameter  $\phi 193.7\text{mm}$  and thickness of 16 mm, supported by a bell-base fixed to a concrete base block. The 4 columns still give support to 6 beam profiles HEB300, 2 disposed in the transverse direction and the 4 remaining one's disposed longitudinally (Silva, 2015) and (Caetano, 2010).

### Description of monitoring sessions

The type of geometry of the structure influences the choice of radar location. For this type of structure the ideal position of the radar is below the bridge deck, because the radar only measures displacements in one direction and the structure displacements required for modal identification are mostly vertical. In addition, since the bridge consists mainly of concrete, its reflectivity to the electromagnetic waves issued by the radar will naturally be more reduced. As a solution, during the execution of the monitoring plan, strategies were also considered for the placement of reflective cones in the structure. The monitoring plan carried out considers two monitoring cases, depending on the arrangement of the reflecting cones (Silva, 2015). In the first case the monitoring is done with the longitudinal distribution of the cones by the two spans; and in the second case, the monitoring is done with the distribution of the cones only in the second span (Figure 2).

Figure 3 shows the placement of the reflecting cones in the area near the deck edge, for which the radar was positioned under the bridge deck also in the vicinity of the deck (Silva, 2015). Such location of the radar also was determined to avoid direct influence on the potential movement of people and vehicles, which could interfere with the opening beam of the radar antennas.



Fig. 3 - Installation of the reflective cones (Silva, 2015)

In Figure 4, the positioning (geometry) of the radar in relation to the bridge is shown, in the direction of monitoring. The geometry that characterizes this monitoring is defined according to the following parameters:

- $x$  represents the horizontal distance (in a straight line) between one end of the bridge and the radar;
- $z$  represents the difference of height between the antennas (starting point of the opening beam) and the bridge deck;
- $\alpha$  represents the aperture of the antennas and varies according to the antenna characteristics;
- $\varphi$  represents the tilt of the radar, in order to obtain a better coverage of the structure with the aperture beam of the antennas.

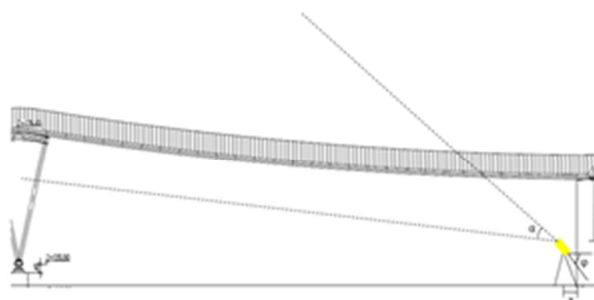


Fig. 4 - Representative diagram (in elevation) of the monitoring geometry from (Silva, 2015)

Table 1 gives the monitoring parameters corresponding to the two monitoring cases (Silva, 2015).

Table 1 - Geometrical Parameters of the Monitoring cases

Cases	X (m)	Z (m)	$\phi$ (degrees)
1	0,60	2,50	20°
2	0,60	2,50	30°

### Analysis and monitoring data comparisons

The choice of radial cells in the first monitoring case was quite satisfactory, since almost all the cones that were placed in the structure presented good results in terms of energy, and which translated into good data for the modal analysis of the structure. In addition to the good results obtained, all the radial cells showed in-phase displacements. As a final result, through the Fourier transform the velocity spectrum of Figure 5 was obtained, in which it was possible to identify the frequencies corresponding to the first and second modes of vibration (Silva, 2015).

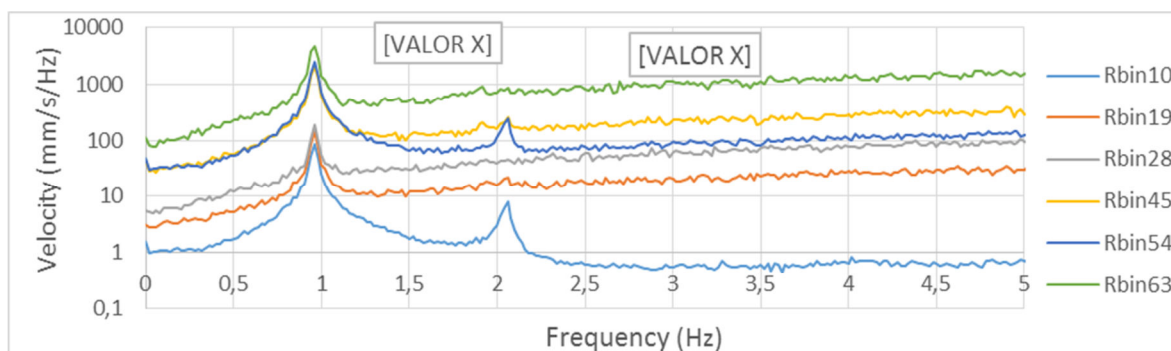


Fig. 5 - Velocity spectrum for the radial cells data selected in the first case from (Silva, 2015)

In the second monitoring case, the location of the reflective cone targets was only on the second span of the bridge; the results obtained were not as good as those of the first case, since of the six cones only four had good displacement signals. Nevertheless the selected radial cells showed in-phase displacements, and through the Fourier transform it was possible to obtain two natural frequencies (corresponding to two modes of vibration: 1st and 3rd) identified in the velocity spectrum of Figure 6.

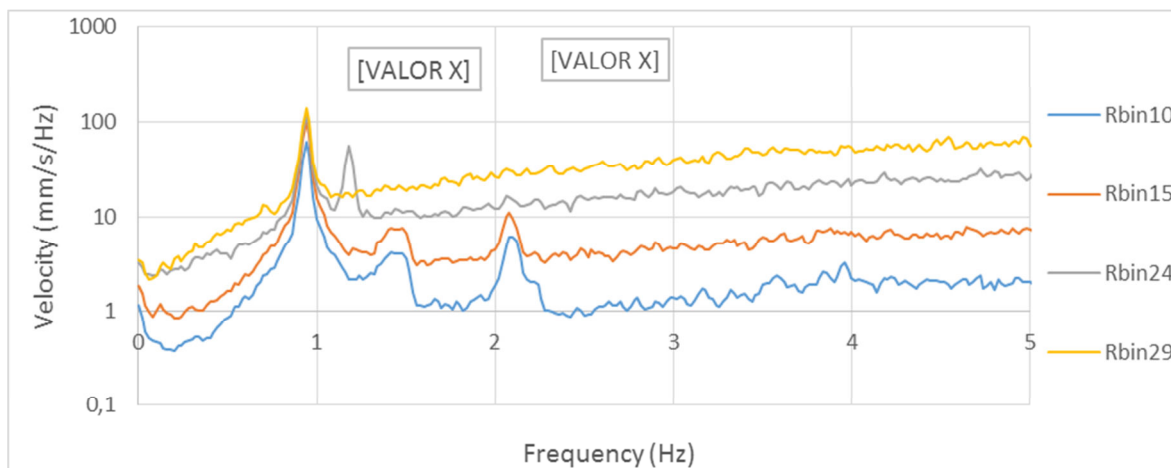


Fig. 6 - Velocity spectrum for the radial cells selected in the second case from (Silva, 2015)

Table 2 shows the values of the bridge natural frequencies identified in the monitoring cases using RI (SHM by RI), and the corresponding frequencies obtained in the well-established Vibest research unit study [6]. The percentual differences are also given, which emphasizes the accuracy of this non-intrusive SHM technique.

Table 2 - Comparison of natural frequencies: SHM by RI and Vibest study

Mode	SHM by RI (Hz)	Vibest Study (Hz)	Difference
1	0,94	0.97	3.1 %
2	2.06	2.04	1.0 %
3	2.08	2.07	0.5 %

## B- Pinhão Bridge

### Structural Description

The Pinhão road bridge (Figure 7) is a structure that allows the crossing of road vehicles through the Douro River, linking the districts of Viseu and Vila Real (Alves, 2016). This is an old structure that was opened to traffic in 1906 and has already undergone a rehabilitation process, notably in 2006, so that it could be able to allow the circulation of road traffic fulfilling all the safety criteria inherent to the current design Eurocodes.



Fig. 7 - Pinhão Bridge from (Alves, 2016)



In structural terms, the steel superstructure consists of a metal deck with three independent span sections spaced 68.60 meters between the supports, and a span (about 10 meters in length) close to the south bridge abutment (Figure 8). The bridge is supported on three pillars (P1, P2 and P3), implanted in the river bed and that present total heights of 20 meters, constructed in granite masonry. The bridge still has two abutments (south abutment and north abutment) also constructed in granite masonry (Alves, 2016).

### Monitoring Considerations for Pinhão Bridge

The monitoring of the Pinhão bridge was carried out in only one bridge span, the northernmost section of the structure (north span, see Figure 8). One of the factors to be taken into account, for the characterization of the dynamic behavior of this span, was the positioning of the radar system. In order to observe the vibration frequencies of the structure in longitudinal and transverse directions, two distinct monitoring operations are carried out in the two directions. The first monitoring refers to the dynamic evaluation of this section with respect to the longitudinal behavior of the bridge; while the second monitoring refers to a dynamic evaluation of the same northernmost deck span with respect to the transversal behavior of the bridge. These RI experimental characterizations are duly explained in the following parts of this subchapter, and are compared with other previous experimental observations obtained by tri-axial accelerometers (using seismographs).

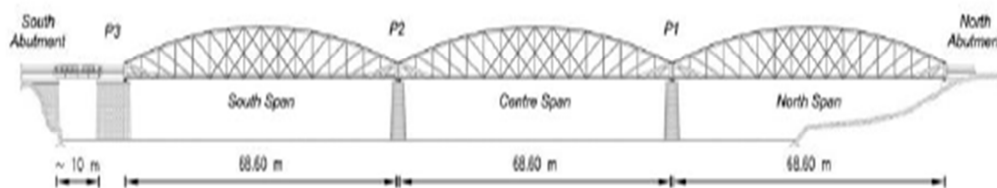


Fig. 8 - Elevation diagram of Pinhão bridge from (Alves, 2016).

### SHM of the longitudinal behavior of Pinhão bridge

For a better identification of the vibration frequencies of the structure in the longitudinal direction, by SHM of the north span bridge section, the IBIS-FS radar is positioned under the bridge deck as shown in Figure 9. This positioning is rational and adequate for the monitoring of bridges and viaducts, since the placement of the radar under a structure of this type allows the observation of vertical displacements that it suffers under environmental actions (causing environmental vibrations) and the circulation of road vehicles from (Alves, 2016).



Fig. 9 - Positioning of radar IBIS-FS for SHM along longitudinal direction from (Alves, 2016).

The number of reflection points in the lower part of the deck has a significant impact on the selection of the measurement points, which can represent good virtual sensors, due to the metallic discontinuities that this structure presents along the span under analysis (Alves, 2016).

From the phase representation it is possible to obtain (from the displacement spectrum in Figure 10) the vibration frequencies of the structure, subjected to environmental actions and road traffic. The data from three radial cells of observations (Rbin 5, Rbin 8, Rbin 13) is quite consistent across the frequency range represented. It can be stated that the data from radial cell Rbin 19 has some discrepancies in this displacement spectrum, relative to the remaining cells; however, because it exhibits practically all of the same vibration frequency peaks, it can be contained in these results (for natural frequencies detection).

Then four vibration frequencies, represented by four frequency peaks (of values equal to 2.84 Hz, 6.44 Hz, 9.78 Hz and 12.96 Hz), are identified by SHM using RI technique. Thus, it can be mentioned that the first observed vertical vibration frequency, equal to 2.84 Hz, corresponds to the first overall bending mode of the structure.

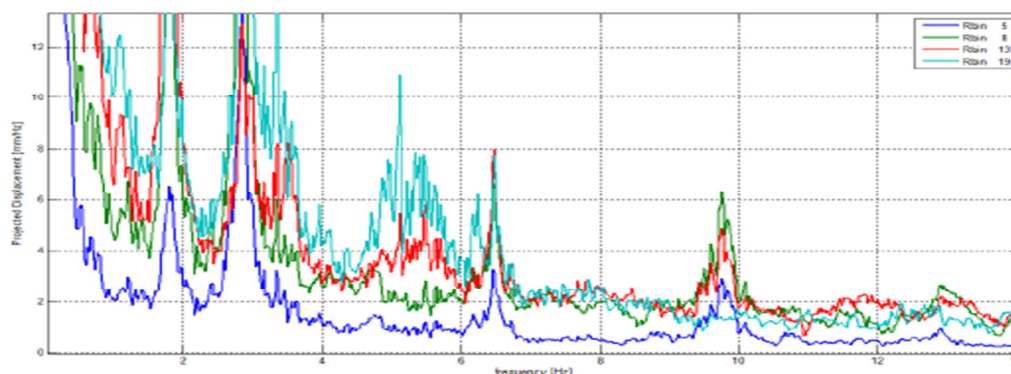


Fig. 10 - Spectrum of projected displacements of the span under analysis by using RI for SHM of the longitudinal bridge behavior from (Alves, 2016).

These results obtained for Pinhão bridge by the RI non-intrusive SHM technique (Figure 10), can be compared with the results associated with the amplitude spectrum of vertical accelerations (Figure 11) obtained through the SHM using tri-axial seismographs implemented after bridge rehabilitation [8]. So Figure 11 identifies the natural frequencies of the span under analysis, at the value of frequency corresponding to the peaks of the vertical accelerations of the structure under environmental vibration tests.

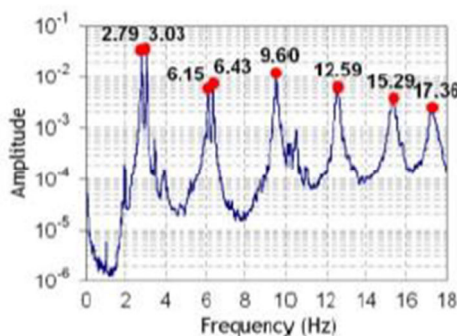


Fig. 11 - Amplitude spectrum of vertical accelerations of the span under analysis obtained by measurements using triaxial seismographs from (Costa, 2012)

Thus it is possible to verify that the results obtained by radar IBIS-FS are consistent with other previous analysis using other SHM techniques, since the first four natural frequencies observed by radar interferometry (RI) [8] are in agreement with similar values obtained by using triaxial seismographs (Costa, 2012).

However, because only the first four vibration frequencies are clearly identifiable, it can be assumed that the quality of the data obtained using RI monitoring technique at this span (at the position selected and without using reflective cones) may have been influenced by the possibility of more than one reflection point in the same resolution cell; thus decreasing the accuracy of frequency acquisition data for subsequent frequency analysis by Fourier transforms. Nevertheless the errors associated with this comparison of SHM techniques, applied for observations in the longitudinal direction, are still identified in Table 3; the accuracy is quite significant.

Table 3 - Comparisons of Longitudinal Natural Frequencies by SHM (Using Seismographs or Using RI) For Pinhão Bridge

Mode	SHM using Seismographs (Hz)	SHM using RI (Hz)	Difference
1	2.79-3.03	2.84	1.8-6.7 %
2	6.15-6.43	6.44	0.1-4.5 %
3	9.6	9.78	1.8 %
4	12.59	12.96	2.9 %

### SHM of the transversal behavior of Pinhão Bridge

The positioning of the radar for observations associated with SHM in transversal direction (Figure 12) is very important, since for this dynamic characterization to be performed the electromagnetic waves generated by the antennas of the radar IBIS-FS have to focus on the horizontal displacements that the structure will exhibit mainly under environmental vibrations.



Fig. 12 - Positioning of radar IBIS-FS for SHM along transversal direction from (Alves, 2016).

Through the spectrum of the projected horizontal displacements (Figure 13), it is possible to obtain the vibration frequencies of the structure in the transverse direction. Thus, two frequencies of peak projected displacements are identified, respectively with values equal to 1.82 Hz and 3.46 Hz. The existence of a higher peak also at 2.84 Hz, coherently indicating the fundamental frequency of the structure in terms of vertical accelerations, clearly means that the positioning of the radar is not that of a purely transverse monitoring of the bridge; therefore, the great sensitivity of the data acquisition using RI, allows to make an additional evaluation of the longitudinal fundamental frequency of bridge vibration.



The analysis of these results of transversal vibrations obtained by SHM using RI (Costa, 2012), can be compared with the amplitude spectrum of transversal accelerations (Figure 14) obtained through the SHM using triaxial seismographs implemented after bridge rehabilitation (Costa, 2012). Table 4 synthesizes such comparison for the first two natural frequencies, indicating the accuracy of these SHM techniques.

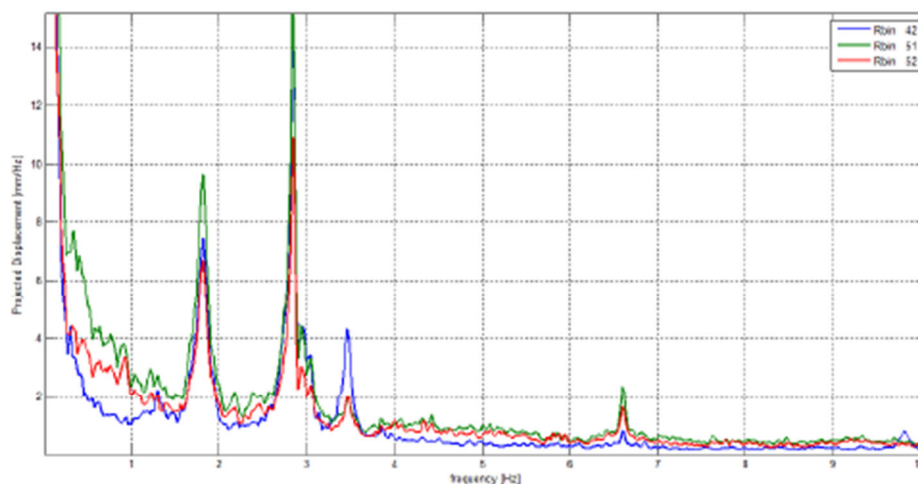


Fig. 13 - Spectrum of projected horizontal displacements of the span under analysis by using RI for SHM of the transversal bridge behavior from (Alves, 2016),

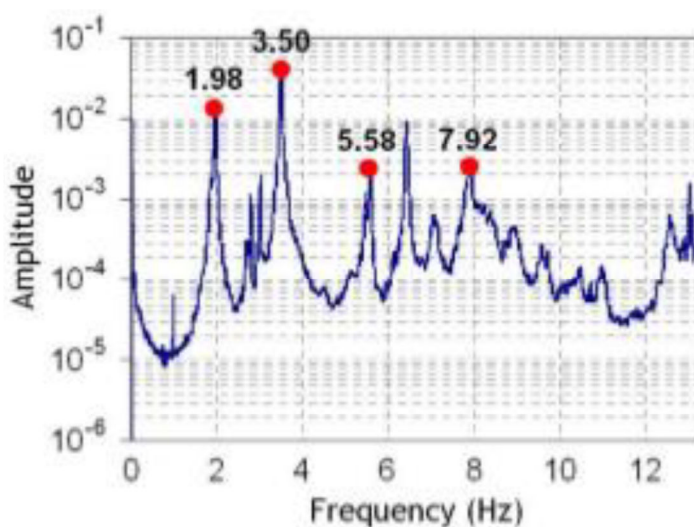


Fig. 14 - Amplitude spectrum of transversal accelerations of the span under analysis obtained by measurements using triaxial seismographs from (Costa, 2012)

Table 4 - Comparisons of Transversal Natural Frequencies by SHM (Using Seismographs or Using RI) For Pinhão Bridge.

Mode	SHM using Seismographs (Hz)	SHM using RI (Hz)	Difference
1	1.98	1.82	8.1 %
2	3.5	3.46	1.1 %

The values in Table 4 are considered close enough, even for the estimation of the fundamental frequency. An estimation of the fundamental transverse frequency with an error of 8.1% is herein considered acceptable, since it was associated with multiple spurious reflections of target points in the same range beam cells, due to unavoidable interference of vehicles traffic on the bridge in the day and during the journey of observations.

### **C- Railway bridge in Alcacer-do-Sal**

The railway bridge in Alcacer-do-Sal promotes the crossing of passenger and freight trains along the Sado River, improving the connections to the south of Portugal and to the port of Sines through a superstructure spanning 2.7 km. It includes a bowstring bridge made of steel and reinforced concrete, about 480 m long, and two access viaducts (north and south) with a total length of 1115 m and 1140 m, respectively (Figure 15). The superstructure is formed by a reinforced concrete deck, supported by metallic components, connected with the piers and foundations also of reinforced concrete (class of resistance C40/50). It was designed for two ballasted railway lines, for trains circulating at a speed up to 240 km/h (Reis, 2010).



Fig. 15 -General view of Alcacer-do-Sal bridge from (Reis, 2010).

In order to take into account the effects caused by the interaction between the track and the structure, the superstructure of these viaducts is divided into sub-decks with continuity in the middle supports. Wherever possible these sub-decks, with middle continuity, are separated in between themselves by simply supported adjacent viaducts (on specific spans) of the full deck. The later also provide a minimization of displacements resulting from temperature changes which the structure is subjected (Reis, 2010) and (Alencar, 2016). For the purpose of SHM, this work therefore refers to a section of the north access viaduct (Figure 16), with a length of 45 m, simply supported at the end piers (which have a height of 10 m).



Fig. 16. Simply supported viaduct of Alcacer bridge under SHM from (Alves,2016)

This simply supported viaduct of the bridge has a cross-section with a 13 meters wide platform throughout its length, supported by two high-rigidity metal beams (2.60 m high, and spaced 5.80 m apart). These beams are interconnected by horizontal diaphragms and bracing systems (Figure 17).

This viaduct section of the bridge, presenting a heavy metallic construction which supports the reinforced concrete slab and the railway line itself, allows a good characterization of its dynamic behavior over time using the radar interferometer system: either through environmental vibrations, and/or through the passage of trains. The discontinuities between the high rigidity metal beams, the connections between the horizontal diaphragms and the bracing, constitute observation points of good electromagnetic reflectivity necessary for the adequate use of the RI on this bridge section (Figure 17) through the IBIS-FS interferometric radar (Alves, 2016).



Fig. 17 - Structural metallic elements (bracing, diaphragms and walkaway) of the viaduct stretch under SHM from (Alves,2016)

The interferometric radar also allows the analysis of the vibration frequencies induced by the Alfa Pendular high-speed train in the railway viaduct span under analysis. In Figure 18 it is represented (for the record Rbin 19, of the observations taken during train passage) the corresponding spectrum of the projected vertical displacements at the position of the reflective cone used underneath the deck. From such spectrum, it is clearly identified the major excitation frequency that such train passage induces in the structure when it circulates at 220 km/h. This excitation is signaled by peak of the projected vertical displacements obtained by the radar at 2.50 Hz. The fundamental frequency of the viaduct span under analysis can also be observed in this displacement spectrum, by the peak at 2.86 Hz. This frequency is associated with the first mode of longitudinal flexural bending vibration of this viaduct span. The presence of several spectrum peaks at frequencies up to 2 Hz, is considered associated with the vibration of the flexible longitudinal metallic walkway (underneath the deck, and not yet monitored with any fixed equipment) under simultaneous environmental excitations and passage of the high-speed train.

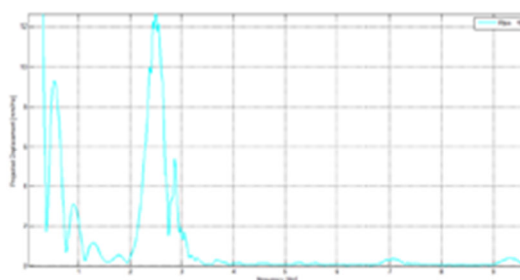


Fig. 18 - Spectrum of projected vertical displacements (using RI) at the section of application of the reflective cone, on the viaduct span under analysis and due to passage of Alfa Pendular train from (Alves, 2016)

The two frequencies mentioned above, obtained by Fourier transform of the observed displacement data when using the IBISDV software (inherent to the IBIS-FS interferometric radar), can also be compared with the corresponding frequencies obtained by the analysis of the displacements data obtained by the Position Sensing Device (PSD) that has been installed in this viaduct span on a steady basis. This PSD is a SHM instrument that detects the variations of the position of a localized point of a structure, through the illumination of a sensor by a laser and detecting variations in the energy of light incident and reflected; this SHM using PSD is part of an investigation to evaluate fatigue effects in the deck slab of this simply supported viaduct of Alcacer bridge (Alencar, 2016).

After MATLAB manipulation of the SHM observations data obtained using PSD, the graph of vibration amplitudes at the sensor point of PSD is obtained (Figure 19), revealing two peaks at frequencies of 2.56 Hz and 2.88 Hz; they correspond to the excitation caused by the Alfa Pendular train passage and to the fundamental frequency of the viaduct span.

Table 5 compares the excitation frequency and the fundamental longitudinal flexural vibration frequency obtained at this viaduct span by the two SHM techniques (PSD and RI). These results confirm that the SHM performed by RI evaluates with great accuracy the precision of the calculations also taken on a steady basis by the PSD, installed in the monitored viaduct for studying specific aspects of the Alcacer bridge dynamics.

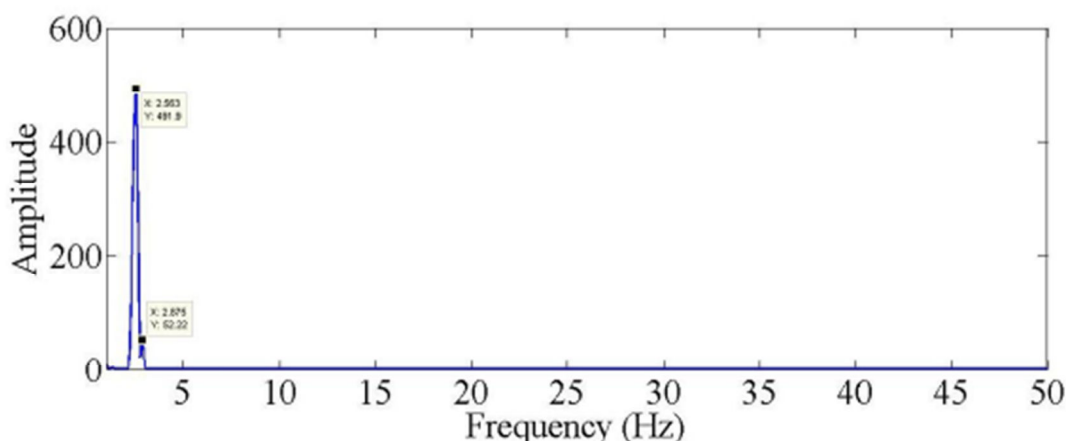


Fig. 19 - Spectrum of vibration amplitudes at sensor point, by PSD system from (Alves,2016)

Table 5 - Comparisons of Frequencies by SHM (Using PSD or Using RI) of Alcacer-do-Sal Bridge.

Peak at spectrum	SHM using PSD (Hz)	SHM using RI (Hz)	Difference
1	2.56	2.50	2.3 %
2	2.88	2.86	0.7 %

## CONCLUSIONS

This article provided dynamic results from SHM using radar interferometry of four practical cases of Portuguese bridges (stress ribbon, metallic and mixed construction) designed for distinct functions (pedestrian, roadway, and railway). The bridges were chosen since they also have been monitored by other techniques. The comparison of results with respect to the evaluation of natural frequencies and excitation frequency, showed the high accuracy the portability and the easiness of use of the radar interferometry non-intrusive technique.

## REFERENCES

- [1] Alencar G, Calçada R, Silva JGS, Jesus AMP. Fatigue Assessment of Approach Viaducts of the New Sado River Railway Crossing. Proceedings of IRF 2016: New trends on Integrity, Reliability and Failure, 1/July/2016, pp.1-17, J.F. Silva Gomes and S.A. Meguid, Porto
- [2] Alves R. Observação Experimental de Estruturas utilizando a Interferometria Laser. Master Thesis, Faculdade de Engenharia da Universidade do Porto, 2016. (*in Portuguese*).
- [3] Barros RC. Desenvolvimento de um Banco de Ensaios para Validação de Apoios Tubulares em Aço de Alta Resistência para Linhas de Transmissão (VHSS-Poles). ISBN: 978-972-752-180-7, FEUP, 2015, p.441.
- [4] Caetano E, Cunha A, Moutinho C., “Vandal loads and induced vibrations on a footbridge”. Journal of Bridge Engineering, 2010. 16(3), pp. 375-382.
- [5] Costa BJA. A. Structural Identification of Old Steel bridges: Monitoring and Rehabilitation Assessment. PhD Dissertation, Faculdade de Engenharia da Universidade do Porto, 2012.
- [6] Gentile C, Bernardini G. Application of Radar Technology to Deflection Measurement and Dynamic Testing of Bridges. IOMAC'09 - 3rd International Operational Modal Analysis Conference, 2010.
- [7] Gentile C. Dynamic measurement on stay-cables using microwave interferometry The radar-based measurement of deflections”. 34th International Symposium on Bridge and Structural engineering, Venice, Italy, 2010.
- [8] Gentile C. Vibration measurement by radar techniques. Proceedings of the 8th International Conference on Structural Dynamics, EUROLYN 2011.



[9] Reis A, Cremer JM, Lothaire A, Lopes N. The steel design for the new railway bridge over the River Sado in Portugal. *Steel Construction* Vol 3 No 4, 2010, pp. 201-211, Ernst & Sohn, Berlin.

[10] Silva L. Monitorização de Estruturas com recurso a Radar Interferométrico. Master Thesis, Faculdade de Engenharia da Universidade do Porto, 2015. (*in Portuguese*).